J Solid State Electrochem (2012) 16:117–126
DOI 10.1007/s10008-011-1292-0

ORIGINAL PAPER

Synthesis, characterization, and thermoelectric properties of a conducting copolymer of 1,12-bis(carbazolyl)dodecane and thieno[3,2-*b*]thiophene

Ruirui Yue · Shuai Chen · Congcong Liu · Baoyang Lu · Jingkun Xu · Jianmin Wang · Guodong Liu

Received: 18 September 2010 / Revised: 8 December 2010 / Accepted: 20 December 2010 / Published online: 20 January 2011

Abstract Poly(1,12-bis(carbazolyl)dodecane-*co*-thieno[3,2-*b*]thiophene) (P(2Cz-D-*co*-TT)), a conducting copolymer was synthesized electrochemically by direct anodic oxidation of 1,12-bis(carbazolyl)dodecane (2Cz-D) and thieno[3,2-*b*]thiophene (TT) in boron trifluoride diethyl ethrate containing 30% (vol) dichloromethane. As-formed copolymers exhibited high redox activity and reversibility and good conductive properties. The emitting property of as-formed copolymer was different from those of respective homopolymers, and could be tuned by changing the initiate monomer feed ratios. Thermoelectric investigations revealed that the electrical conductivities of as-obtained copolymer films were between 0.1 and 0.3 S cm^{-1} at ambient temperature, lower than that of polythieno[3,2-*b*]thiophene (PTT) (0.42 S cm^{-1}) but two orders of magnitude higher than that of poly(1,12-bis(carbazolyl)dodecane) (P2Cz-D) (10^{-3} S cm^{-1}). The Seebeck coefficients and the power factors of the copolymers were improved with different degrees compared with those of PTT and P2Cz-D. As expected, the thermoelectric performance of PTT and P2Cz-D were both improved through copolymerization, which may be beneficial to the exploration and investigation of novel organic thermoelectric materials.

Keywords Conducting polymers · Electrochemical copolymerization · Thermoelectric material · Polythiophene · Polycarbazole

R. Yue · S. Chen · C. Liu · B. Lu · J. Xu (✉)
Jiangxi Key Laboratory of Organic Chemistry,
Jiangxi Science and Technology Normal University,
Nanchang 330013, China
e-mail: xujingkun@tsinghua.org.cn

J. Xu
e-mail: xujingkun@mail.ipc.ac.cn

J. Wang · G. Liu
School of Communication and Electronics,
Jiangxi Science and Technology Normal University,
Nanchang 330013, China

Introduction

Thermoelectric materials have been of great interest from the viewpoint of applications in both power generation and solid-state cooling or heating. The thermoelectric power generation could be widely used as special power source and as novel energy harvesting systems, such as waste heat recovery and high efficiency solar energy conversion. Solid cooling or heating using thermoelectric technology has done great contributions to developing frontier electronic devices [1–3]. Until recently, most investigations for thermoelectric materials focused on inorganic compounds, such as bismuth telluride [4], skutterudites [5], half-Heusler alloys [6], clathrate compounds [7], and pentatellurides [8]. However, the relatively high cost and poor processability of these inorganic semiconductor thermoelectric materials are impeding their spreading applications to many new thermoelectric systems [9]. Therefore, it is timely and necessary to explore novel thermoelectric materials with high performance and low cost and to seek economical way to manufacture thermoelectric devices.

Compared with inorganic semiconducting materials, conducting polymers have attractive features for using as thermoelectric materials including potential low cost due to abundance of carbon resources, low density, easy synthesis, and easy processing into versatile forms. Furthermore, their

low thermal conductivity is generally expected to be advantageous for enhancing thermoelectric properties in terms of the performance of a thermoelectric material evaluated by its dimensionless figure-of-merit, $ZT = (S^2\sigma)T/\kappa$ (S, σ, κ, and T are Seebeck coefficient, electrical conductivity, thermal conductivity, and absolute temperature, respectively). This implies that polymer thermoelectrics could become competitive, even if their efficiency is less than that of current semiconductor materials. Until now, the thermoelectric research based on conducting polymers mainly focus on polythiophenes [10–12], polycarbazoles [13–15], polyanilines [3, 16] polyphenylenevinylenes [17, 18], polypyrroles [19], and their composites with other organic/inorganic materials [3, 10–12, 16, 20, 21]. As reported, some of them show thermoelectric properties comparable to those of conventional inorganic thermoelectric materials. Since for these conjugated polymers, it is a wise way to achieve and improve various properties via adjusting the electronic character of the π-orbit along the polymer backbone, including main chain and pendant group structural modification, composite with other organic or inorganic materials, and copolymerization [11, 22–25].

As a general synthetic method, copolymerization is a promising strategy to obtain materials with combining properties of the constituent homopolymers. Carbazole containing polymers are of interest due to their various advantageous properties, such as high charge carrier mobility, high thermal and photochemical stability, and their applications in electrochromic devices, hole transport layers, electro-xerography, microcavity photoconduction, and as photo-voltaic components that provide a very efficient matrix as a current carrier transport [26–34]. On the basis of previous theoretical band structure calculations on some polycarbazole derivatives, it is reported that polycarbazole derivatives usually exhibit high Seebeck coefficients [13]. Therefore, we wish to main a high Seebeck coefficient while improving the electrical conductivity. Recently, dicarbazoles connected with various ether-oxide spacers [35, 36], biphenyl [37], and carbon chains [38] have been investigated, such as 1,12-bis(carbazolyl) dodecane (2Cz-D) [38]. Due to the ease of formation of relatively stable radical cations (polarons), carbazole readily polymerize at electrochemical polymerization process. As reported previously [38], poly(1,12-bis(carbazolyl)dodecane) (P2Cz-D) films synthesized electrochemically exhibit good emitting properties and high mechanical property, due to the increased polymerization positions and the introduction of flexible carbon chains and that crosslinking structures can be easily formed during the polymerization process. However, up to our knowledge, there is little study on the thermoelectric property of P2Cz-D reported, which may be attributed to its reported relatively lower electrical conductivity (10^{-3} S cm^{-1}). Therefore, the electrical conductivity of P2Cz-D should be improved to ascertain that P2Cz-D can be used as thermoelectric material. On the other hand, polythieno[3,2-*b*]thiophene (PTT) as a derivative of polythiophenes has been already reported by our group as one thermoelectric material [39]. The rigid π-conjugated structure and the easy synthesis of conducting polymer films with relatively high electrical conductivity indicate that thieno[3,2-*b*]thiophene (TT) may be one proper comonomer for 2Cz-D to achieve a novel copolymer with improved electrical conductivity and Seebeck coefficient.

Here, we report the synthesis of a conducting copolymer of 2Cz-D and TT via electrochemical copolymerization (Scheme 1). Considering the easy synthesis of high-quality polymer films in boron trifluoride diethyl ethrate (BFEE) and the good solubility of 2Cz-D in dichloromethane (DCM), a binary solvent electrolyte containing 70% (vol) BFEE and 30% (vol) DCM was chosen for this experiment. The electrochemical behavior, structural characterization, optical properties, thermoelectric performance, and morphologies of as-formed poly(1,12-bis(carbazolyl)dodecane-*co*-thieno[3,2-*b*]thiophene) (P(2Cz-D-*co*-TT)) films were investigated in detail.

Experimental section

Chemicals

2Cz-D and TT were synthesized according to the general procedures already described [40, 41]. BFEE (AR, Beijing Changyang Zhenxing Chemical Plant, China), dichloromethane (DCM), tetrahydrofuran (THF), and *N*,*N*-

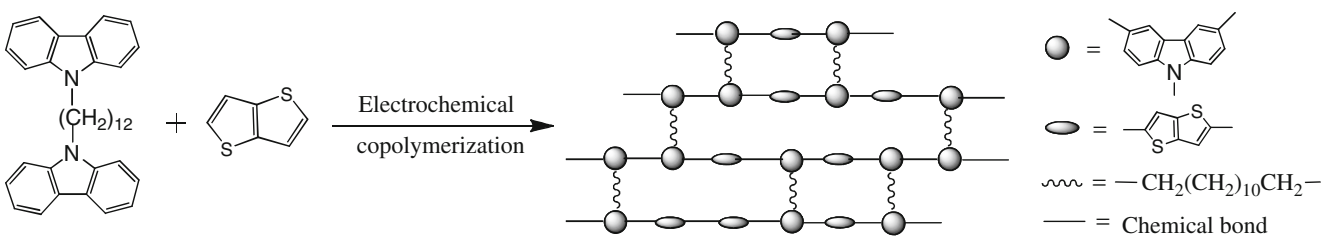

Scheme 1 Electrochemical copolymerization reaction of 2Cz-D and TT

dimethylformamide (DMF, AR, Beijing Chemical Plant, China) were distilled before use. Carbazole and 1,12-bisbromododecane (Acros Organics), diisopropylamine, *N*-formylpiperidine and ethyl 2-sulfanylacetate (AR, Shanghai Zhuorui Chemical Plant, China), *n*-butyllithium (Shangyu Hualu Chemical Co., Ltd., Zhejiang, China), NH_4Cl (AR, Beijing Chemical Plant, China), quinoline (AR, Beijing Xizhong Chemical Plant, China), K_2CO_3, dimethylsulfoxide, and $LiOH{\cdot}H_2O$ (AR, Tianjin Hengxing Reagents Factory, China), and copper powder (99.5%, AR, Tianjin Bodi Chemical Co., Ltd., China) were all used without further purification.

Electrochemical synthesis and test

Electrochemical polymerization and examination were carried out in a one-compartment three electrodes cell with a Model 263 potentiostat-galvanostat (EG&G Princeton Applied Research) under computer control at room temperature. The working and counter electrodes for cyclic voltammetry (CV) experiments were two platinum wires with diameter of 0.5 mm, respectively, placed 0.5 cm apart. Before each examination, they were carefully polished and cleaned with water and acetone successively. All solutions were deaerated by a dry argon stream before experiments. An Ag/AgCl electrode immersed directly in the solution was used as the reference electrode. A correction of 0.069 V is needed to bring the measured potentials in the binary solvent solution originally vs. Ag/AgCl to potentials vs. the standard hydrogen electrode [42]. To obtain free-standing polymer films, a platinum sheet with surface area of 4.5 cm^2 and a stainless steel sheet with surface area of 6.0 cm^2 were employed as the working and counter electrodes, respectively, and they were carefully polished with abrasive paper (1500 mesh) and then washed with water and acetone successively before each examination. The polymers deposited on indium tin oxide (ITO) glasses (about 2.0 cm^2) were used for UV-vis, fluorescence, and morphologies measurements. For special analysis, the as-formed polymers were de-doped with 25% ammonium for 3 days and then washed repeatedly with water and acetone. At last, they were dried at 60°C for 2 days in vacuum.

Characterization

The temperature dependence of electrical conductivity (σ) and Seebeck coefficient (S) were measured by a four-point measurement unit of thermoelectric properties coupled with a liquid nitrogen container for rectangular shaped film samples (length 12.0–13.0 mm, width 3.0–3.5 mm, thickness 0.03–0.10 mm) from room temperature to 200 K. Seebeck coefficient was obtained from the slop of the produced thermoelectric voltage as a function of the temperature difference along the length of the sample. The power factor ($P=S^2\sigma$) was calculated from the corresponding Seebeck coefficient and electrical conductivity at a certain temperature.

UV-vis spectra were measured with a Perkin-Elmer Lambda 900 UV-visible-near-infrared spectrophotometer. With an F-4500 fluorescence spectrophotometer (Hitachi) fluorescence spectra were determined. Infrared spectra were recorded with a Bruker Vertex 70 Fourier transform infrared (FT-IR) spectrometer with samples in KBr pellets. A VEGA \\LSU TESCAN scanning electron microscope (SEM) was used to analysis the surface morphologies of the as-formed polymer films.

Results and discussion

Electrochemical copolymerization of 2Cz-D and TT

To determine whether the copolymerization of 2Cz-D and TT be feasible, the onset oxidation potentials of the monomers were first studied. As Fig. 1 shows, the onset oxidation potentials of TT (a) and 2Cz-D (b) were 0.80 and 0.46 V, respectively. Besides the onset oxidation potentials of the monomers, the initial feed ratios of the monomers also play an indispensible role in the copolymerization process. According to the strategy of diffusion method established by Kuwabata et al. [43], the monomer with low oxidation potential can be oxidized under diffusion limiting condition at the potentials where the oxidation of higher oxidation potential monomer takes place. Thus, a series of experiments with different initial monomer feed ratios were

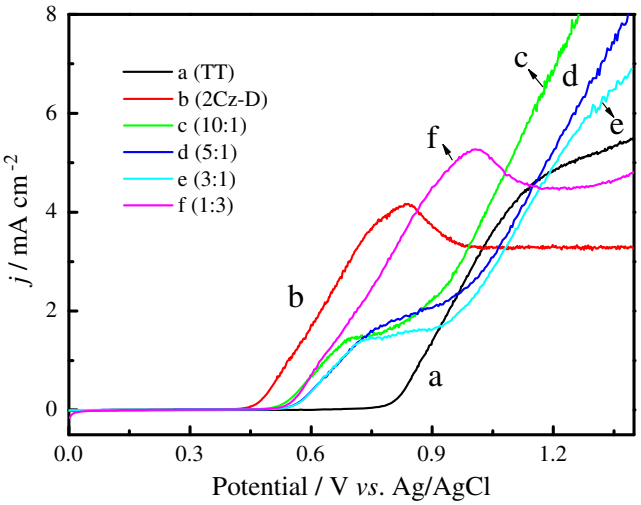

Fig. 1 Anodic polarization curves of TT (**a**), 2Cz-D (**b**), and monomer mixtures with feed ratios of TT/2Cz-D=10:1 (**c**), 5:1 (**d**), 3:1 (**e**), and 1:3 (**f**) in BFEE + DCM (30%, vol). Potential scan rate 20 mV s^{-1}

carried out for comparison and to optimize a suitable monomer feed ratio for the copolymerization process. From Fig. 1(c–f), the onset oxidation potentials of the monomer mixtures with different feed ratios mainly focused on 0.50–0.55 V between those of 2Cz-D and TT. Therefore, it can be easily deduced that the radical cations of 2Cz-D and TT can form almost simultaneously at the working electrode surface where they can react with each other and form a copolymer [44].

The polymer growth and electrochemical behavior can be monitored and followed by cyclic voltammetry. Therefore, the CVs for the electropolymerization processes of 2Cz-D, TT, and 2Cz-D/TT mixtures are shown in Fig. 2. From the CVs, it can be observed that the growth of the conducting polymers clearly appears as reversible or irreversible peak current density increases on each coming CV. Figure 2(a) shows the CVs of 2Cz-D which was performed between −0.2 and 0.7 V. Upon repeated scanning, a reversible redox process develops at about 0.4 and 0.1 V, signifying the formation of an electroactive polymer. However, as CV scanning continued, obvious potential shift of the redox waves appeared, providing information about the increase in the electrical resistance of the formed polymer film and overpotential needed to overcome the resistance [45]. Moreover, the redox peak current density in Fig. 2(a) increased at first and then decreased as the CV scanning continued indicating the poor electrochemical activity and stability. Figure 2(f) displays the CVs of TT with broad redox peaks at 0.6 and 0.1 V and the redox peak current density increased gradually as the CV scanning continued. Figure 2(b–e) shows the CVs of the monomer mixtures with different feed ratios. Compared with the CVs of 2Cz-D and TT Fig. 2(a, f), new redox peaks appeared in the CVs of the monomer mixtures Fig. 2(b–e), suggesting the two monomers were oxidized simultaneously and the copolymerization between them happened. Moreover, as the monomer feed ratio (TT/2Cz-D) increased from 1:3 to 10:1 Fig. 2(b–e), the corresponding CVs became more and more similar to that of TT, indicating more TT units inserted into the copolymer backbone chain.

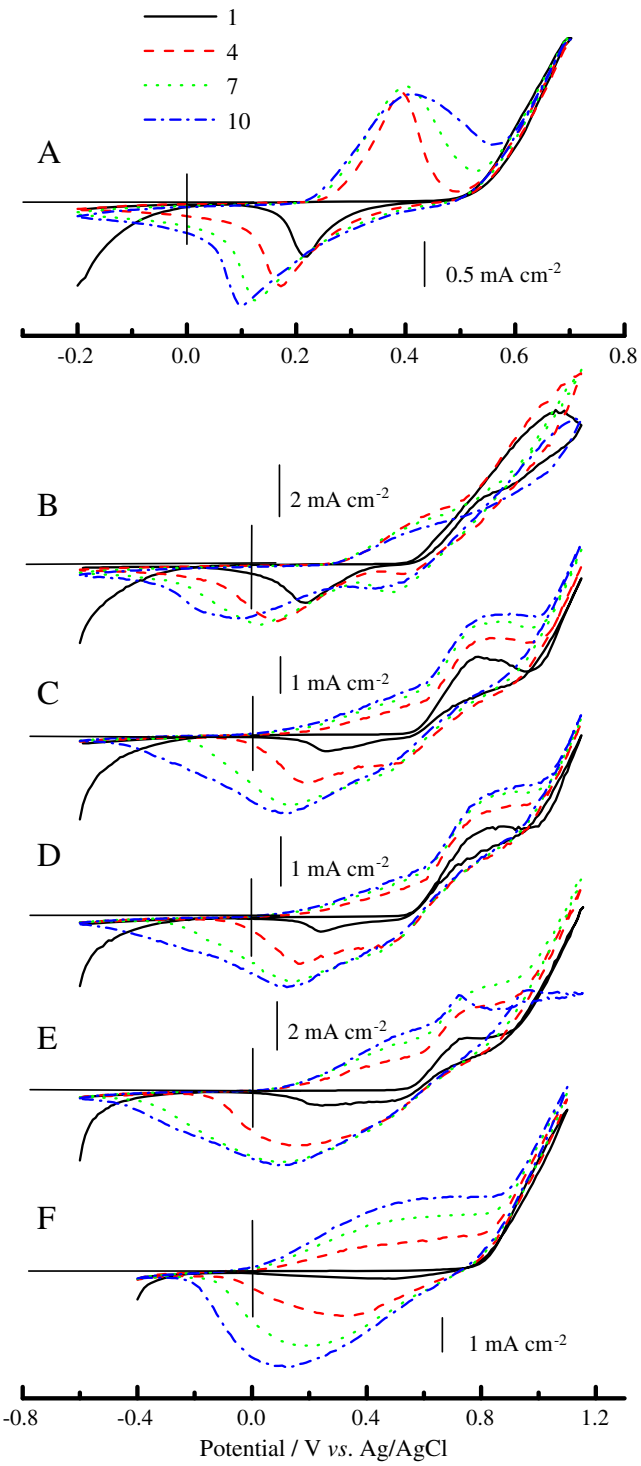

Fig. 2 CVs (the 1st, 4th, 7th, and 10th cycles) of 2Cz-D (**a**), TT (**f**), and monomer mixtures with feed ratios of TT/2Cz-D=1:3 (**b**), 3:1 (**c**), 5:1 (**d**), and 10:1 (**e**) in BFEE + DCM (30%, vol). Potential scan rate 100 mV s^{-1}

Electrochemistry of P(2Cz-D-*co*-TT) films

To obtain high quality polymer/copolymer films, different applied potentials were introduced to ascertain the optimum potentials for polymerization/copolymerization processes under potentiostatic mode, and the chronoamperometric curves of 2Cz-D, TT, and monomer mixtures were recorded. The chronoamperometric curves of the monomer mixture were shown in Fig. 3. According to the chronoamperometric curves and considering the overall factors affecting the quality of as-formed polymer films, such as polymerization rate, unavoidable over-oxidation, room temperature, and adherence against the electrode surface, the chosen applied polymerization potentials are 0.75 V for 2Cz-D, 0.90 V for TT, and 0.95 V for the monomer mixtures with different feed ratios in BFEE + DCM (30%, vol).

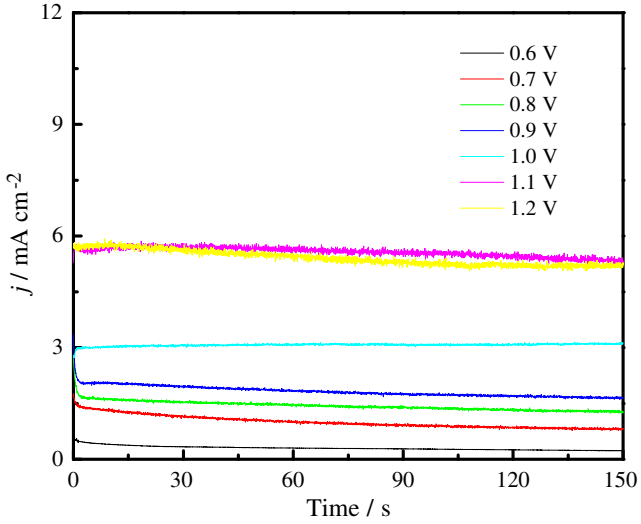

Fig. 3 Chronoamperometric curves of the monomer mixture with TT/2Cz-D=5:1 in BFEE + DCM (30%, vol) on a Pt electrode at different applied potentials for 150 s

The electrochemical behavior of as-formed P(2Cz-D-*co*-TT) film was investigated by CVs under different potential scan rates compared with those of P2Cz-D and PTT films, as shown in Fig. 4. All the polymer films were potentiostatically coated on platinum wires from respective quiescent binary solvent solutions at ambient temperature for 50 s, respectively. P2Cz-D was obtained from the solution containing 0.1 M 2Cz-D at applied potential of 0.75 V, and PTT was synthesized from the solution with 0.1 M TT at applied potential of 0.90. While for P(2Cz-D-*co*-TT) film, it was obtained from the solution containing 0.25 M TT and 0.05 M 2Cz-D at applied potential of 0.95 V. Figure 4(a) displays the CVs of P2Cz-D film, which exhibited two pairs of obvious redox peaks at 0.7 (anodic peak potential, E_{pa}) and 0.5 (cathodic peak potential, E_{pc}) V and 0.4 (E_{pa}) and 0.1 (E_{pc}) V. Figure 4(b) shows the CVs of PTT film, broad redox peaks can be seen at 0.6 (E_{pa}) and 0.1 (E_{pc}) V. The CVs of P(2Cz-D-*co*-TT) film were shown in Fig. 4(c). As the CVs show, broad waves with two pairs of redox peaks can be observed (E_{pa} 0.74 V, E_{pc} 0.36 V; E_{pa} 0.45 V, E_{pc} 0.10 V) due to the overlap of the redox peaks of P2Cz-D (two pairs of redox peaks) and PTT (broad redox peaks), indicating the presence of both the 2Cz-D and TT units in the copolymer backbone chains, as Scheme 1 shows. From Fig. 4, the CVs for P2Cz-D, PTT, and P(2Cz-D-*co*-TT) films can be cycled repeatedly under the potential scan rate from 300 to 25 mV s^{-1}, respectively, exhibiting obvious and similar redox peaks between adjacent CV circles. On the other hand, these films could be cycled repeatedly between the conducting (oxidized) and insulating (neutral) state without significant decomposition of the materials, which could be also observed visually and mainly by virtue of their long and stable π-conjugated

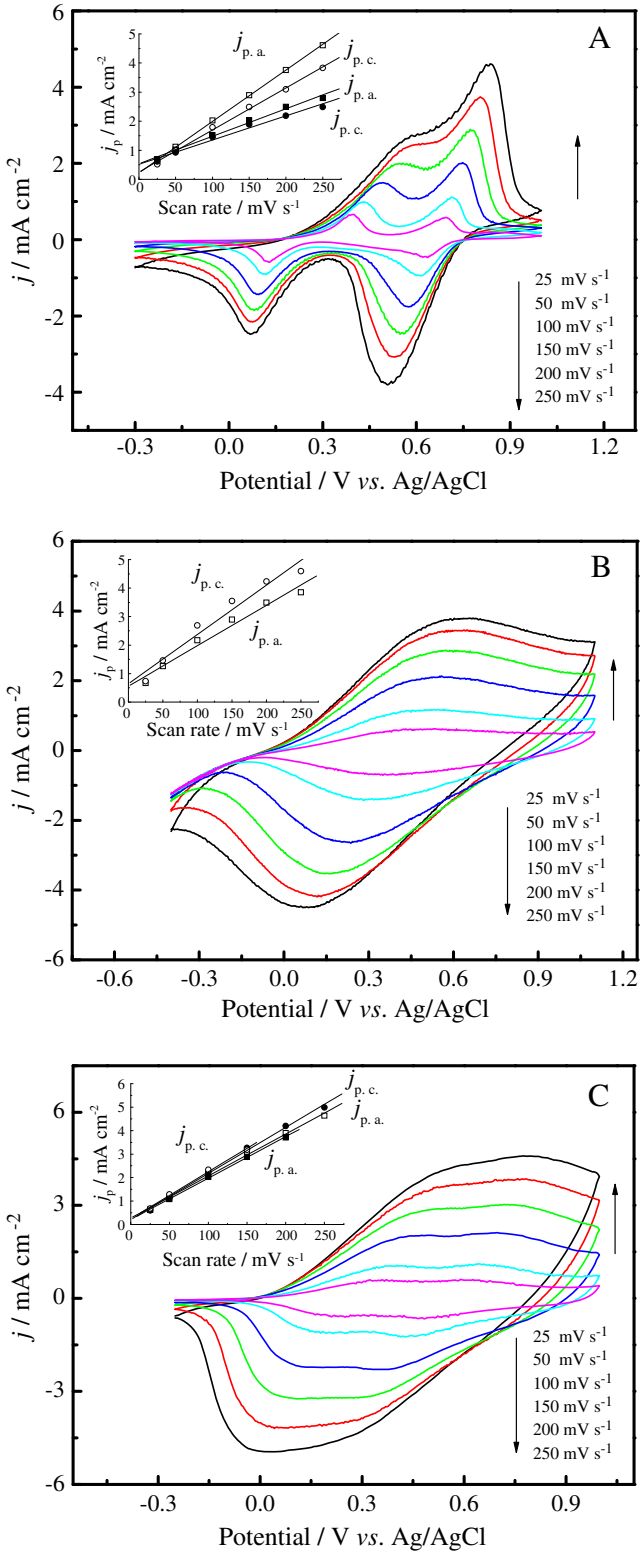

Fig. 4 CVs of P2Cz-D (**a**), PTT (**b**), and P(2Cz-D-*co*-TT) (TT/2Cz-D=5:1) (**c**) films recorded in monomer-free BFEE + DCM (30%, vol) at different potential scan rates indicated. *Insets* plots of redox peak current densities vs potential scan rates. *j* is peak current density, and $j_{p.a.}$ and $j_{p.c.}$ denote the anodic and cathodic peak current densities, respectively

structure. All the results suggest the high structure stability, high electrochemical stability, and good redox activity of the polymer/copolymer films [24, 38, 39, 46, 47]. The scan rate dependence of P2Cz-D, PTT, and P(2Cz-D-*co*-TT) films were also investigated (insets in Fig. 4), respectively. As the insets in Fig. 4 show, a linear relationship was found between the peak current density and the scan rate, indicating that the electroactive polymer film was well adhered to the electrode surface and the redox processes were non-diffusion limited [46–48].

Spectral characterizations

Since both 2Cz-D and TT can be facilely electrodeposited and corresponding polymers with relatively long backbone chain and broad π-conjugated structure are usually achieved through electrochemical method, thus as-formed P2Cz-D, PTT, and P(2Cz-D-*co*-TT) exhibited poor solubility in common organic solvents, such as dichloromethane, chloroform, and dimethyl sulfoxide. In this part, the structural and optical properties of P(2Cz-D-*co*-TT) together with those of P2Cz-D and PTT were characterized by FT-IR, UV-vis, and fluorescence spectra.

The FT-IR spectra of P(2Cz-D-*co*-TT) deposited from different monomer feed ratios, P2Cz-D, and PTT were shown in Fig. 5. For PTT (a), the band at 3078 cm^{-1} is ascribed to the =C–H stretching vibration of heterocycle. The bands at 1,609 and 1,407 cm^{-1} are assigned to the C=C vibration and the bands at 1,330 and 791 cm^{-1} belong to the C–H deformation vibration. The C–C stretching vibration is presented at 1,152 cm^{-1} and the band at

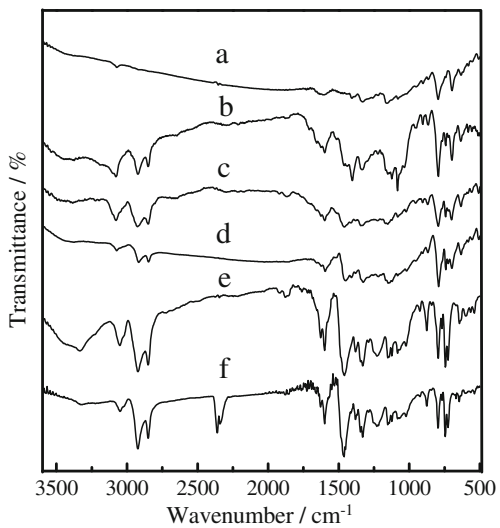

Fig. 5 FT-IR spectra of PTT (**a**), copolymers deposited with monomer feed ratios of TT/2Cz-D=10:1 (**b**), 5:1 (**c**), 3:1 (**d**), and 1:3 (**e**), and P2Cz-D (**f**) in de-doped state from BFEE + DCM (30%, vol)

697 cm^{-1} is assigned to the C–S–C stretching vibration [49, 50]. For P2Cz-D (f), the band at 3,048 cm^{-1} is ascribed to the C–H stretching vibration of benzene rings. The bands at 2,922 and 2,850 cm^{-1} are attributed to the aliphatic C–H stretching vibration, and at 1,600 and 1,465 cm^{-1} are assigned to C=C stretching vibration of benzene rings. The vibration bands at 874, 800, and 745 cm^{-1} indicate the emergence of 1,2,4-tri-substituted benzene ring. For the copolymers (b–e), bands at 3,078, 2,927, 2,849, 881, and 743 cm^{-1} can be still observed, indicating the presence of 2Cz-D units in the copolymers. Moreover, as the initiate monomer feed ratio (TT/2Cz-D) increased from 1:3 to 10:1, the absorption intensity at 2,927, 2,849, 881, and 743 cm^{-1} diminished relatively, suggesting fewer 2Cz-D units inserted into the copolymer main chain, while the enhanced bands at 3,078 and 697 cm^{-1} implied the appearance of TT units in the copolymer main chains. The above-depicted further indicates the occurrence of the copolymerization of 2Cz-D and TT in BFEE + DCM (30%, vol). Furthermore, according the studies reported previously that the electrochemical polymerization of carbazole and its derivatives mainly occurred at 3,6 positions [51]; thus, it can be reasonably deduced that the copolymerization of 2Cz-D with TT still occurred at its 3,6 positions.

Figure 6(a) depicts the UV-vis spectra of P2Cz-D, PTT, and P(2Cz-D-*co*-TT) in solid phase (ITO glass surface). UV-vis spectrum of PTT exhibits an absorption band with a maximum at 468 nm attributed to the π–π* transition along the polymer chain and a broad band centered at 700 nm attributed to the absorption of conductive species such as polarons and bipolarons. While for P2Cz-D, the UV-vis spectrum shows an absorption band at 396 nm induced by the π–π* transition of carbazole moiety and a broad band at 825 nm attributed to the absorption of polarons or bipolarons. After copolymerization of 2Cz-D and TT, as-formed copolymers synthesized with TT/2Cz-D=10:1, 5:1, and 3:1, show absorption band at 396 nm and broadbands at about 540 and 580–980 nm, different from those of P2Cz-D and PTT. For the copolymer backbone structure, it can be seen as that TT units were inserted into P2Cz-D main chains as little bridges between two adjacent and uncombined 2Cz-D units to improve the regularity of the polymer backbone chains. However, the continuity and effective conjugation length of PTT segments in the copolymer main chain were damaged simultaneously compared with that of pure PTT. Thus, the absorption of TT/PTT moiety in the copolymer backbone chain was effected and different from that of PTT.

The fluorescence spectra of P2Cz-D, PTT, and P(2Cz-D-*co*-TT) films deposited on ITO glass electrode were shown in Fig. 6(b). As literature reported [38], P2Cz-D is good blue-light emitter with a strong emitting peak at 420 nm and shoulder peaks at 400, 442, and 468 nm, which may be

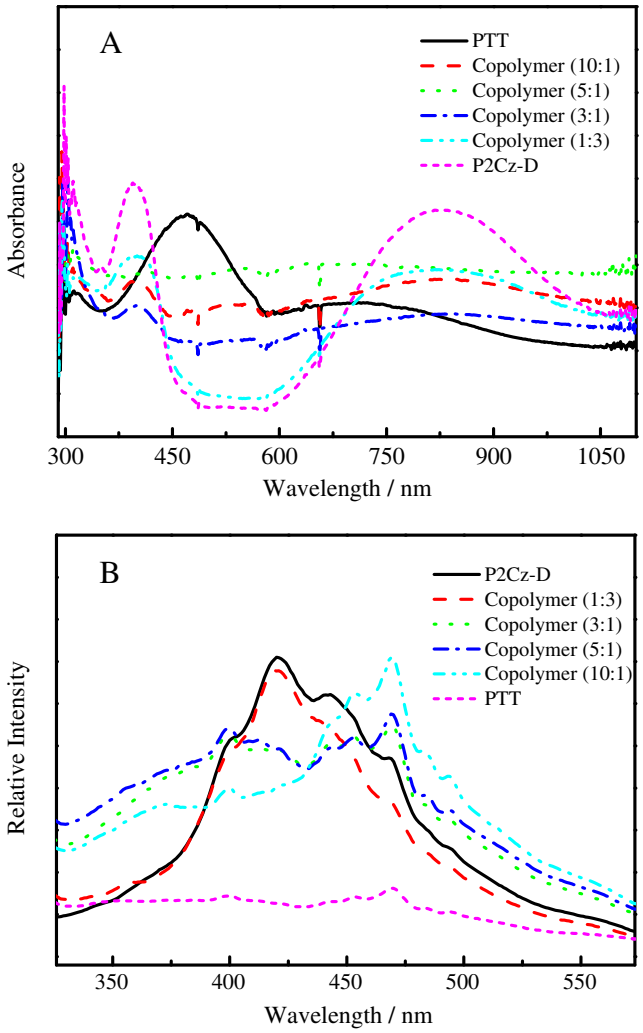

Fig. 6 UV-vis spectra (**a**) and emission spectra (**b**) of doped P2Cz-D, PTT, and copolymer films deposited with feed ratios of TT/2Cz-D= 10:1, 5:1, 3:1, and 1:3 on ITO glasses in BFEE + DCM (30%, vol)

attributed to the different conjugation length of polycarbazole (PCz) chains. The emitting spectrum of P(2Cz-D-*co*-TT) copolymerized with TT/2Cz-D=1:3 was similar with that of P2Cz-D, indicating few TT units were inserted into the copolymer main chains. As the monomer feed ratios (TT/2Cz-D) increased to 3:1, 5:1, and 10:1, much changes occurred to the emitting spectra of as-obtained copolymers. As the figure shows, there were two main emitting peaks at 400 and 469 nm with shoulder peaks at 413 nm and 442, 453, 483, and 494 nm, respectively, implying wider dispersion of the conjugation length of PCz moiety in the copolymer main chains compared with that of P2Cz-D. Since PTT films performed poor fluorescence property, the presence of TT moiety in the copolymer backbone chain destroyed the original conjugation structure of P2Cz-D, and consequently caused fluorescence quenching. The above-depicted also certified the occurrence of the copolymerization between 2Cz-D and TT and the general structure of the copolymer as Scheme 1 exhibited.

Thermoelectric property

As our previous studies reported [38, 39], both 2Cz-D and TT can be formed in high quality free-standing P2Cz-D and PTT films through electrochemical polymerization. In the present study, free-standing P(2Cz-D-*co*-TT) films with high quality and flexibility can be facilely obtained electrochemically in ambient temperature. As-formed free-standing P(2Cz-D-*co*-TT) film with smooth and glossy surface can be peeled off the platinum sheet directly by hand and can be cut into any shapes with a pair of scissors (Fig. 7).

The temperature dependence of electrical conductivities of P2Cz-D, PTT, and P(2Cz-D-*co*-TT) films deposited under different monomer feed ratios were measured and shown in Fig. 8. As temperature decreased from 300 to 200 K, all the measured electrical conductivities decreased gradually, a typical behavior of semiconducting materials [14, 17]. The electrical conductivity of PTT in ambient temperature was 0.42 S cm^{-1} lower than that (1.5 S cm^{-1}) reported previously by our group [39], which may be attributed to that the binary solvent electrolyte caused lower doped-degree of PTT films compared with that in pure BFEE. As the temperature decreased to 200 K, the electrical conductivity of PTT film decreased gradually to 0.04 S cm^{-1} one order of magnitude lower than that in ambient temperature. For P2Cz-D film, its electrical conductivity was 1.6×10^{-3} S cm^{-1} at ambient temperature and decreased to 3.8×10^{-5} S cm^{-1} at 200 K. As different amounts of TT units inserted into P2Cz-D main chains, the electrical conductivities of obtained copolymer films were improved with different degrees. The electrical conductivity

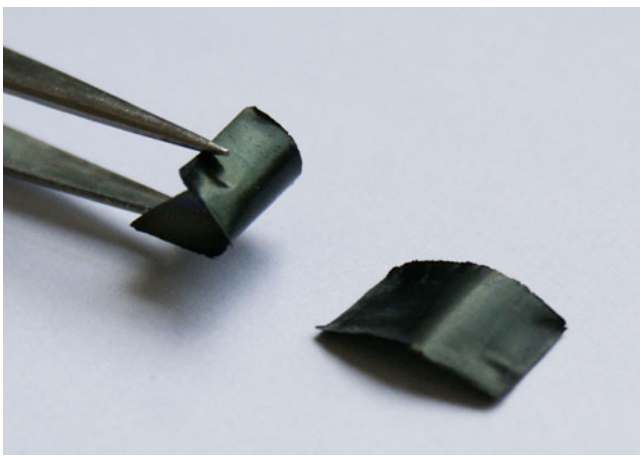

Fig. 7 Photograph of as-formed free-standing P(2Cz-D-*co*-TT) films deposited from monomer mixture with initiate feed ratio of TT/2Cz-D=5:1 at 0.95 V

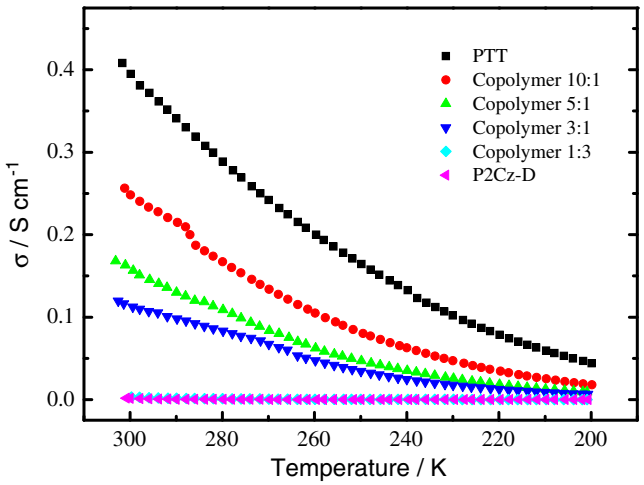

Fig. 8 Temperature dependence of electrical conductivities for PTT, P2Cz-D, and copolymers synthesized with monomer feed ratios of TT/2Cz-D=10:1, 5:1, 3:1, and 1:3 in BFEE + DCM (30%, vol)

of P(2Cz-D-*co*-TT) film synthesized with initiate TT/2Cz-D=1:3 was 3.0×10^{-3} S cm^{-1} at ambient temperature and decreased to 4.0×10^{-5} S cm^{-1} at 200 K, showing a little improvement compared with that of P2Cz-D film. Then, as the initiate monomer feed ratios increased from TT/2Cz-D=3:1 to 10:1, apparent increase in the electrical conductivities of the copolymer films can be observed. For P(2Cz-D-*co*-TT) films deposited from TT/2Cz-D=3:1 and 5:1, their room temperature electrical conductivities were 0.12 and 0.17 S cm^{-1}, respectively, which were lower than that of PTT but higher than that of P2Cz-D by two orders of magnitude. When the initiate monomer feed ratio increased to TT/2Cz-D=10:1, the electrical conductivity of as-formed copolymer film increased to 0.26 S cm^{-1}, indicating that more TT units inserted into the copolymer backbone chains and the conjugation structure together with the regularity of the copolymer main chains was enhanced compared with that of P2Cz-D.

Although the presence of 2Cz-D units in the copolymer backbone chains show negative effect to the electrical conductivities of the copolymers, it is exactly beneficial to improve the Seebeck coefficients of these copolymer films. As Fig. 9(a) shows, the Seebeck coefficient of PTT film was about 75 μV K^{-1} at room temperature and gradually decreased to 51 μV K^{-1} as the temperature decreased to 200 K. The Seebeck coefficient of P(2Cz-D-*co*-TT) film deposited with TT/2Cz-D=10:1 was 85 μV K^{-1} at ambient temperature and 66 μV K^{-1} at 200 K higher than that of PTT (Fig. 9(a)), but the calculated power factor ($P=S^2\cdot\sigma$) was 0.18 μW m^{-1} K^{-2} lower than that of PTT (0.23 μW m^{-1} K^{-2}) at 301 K (Fig. 9(b)). As the monomer feed ratio decreased to TT/2Cz-D=5:1 and 3:1, the Seebeck coefficients of as-obtained copolymer films were about 143 and 169 μV K^{-1} at 305 K, respectively, much higher than those of PTT and P(2Cz-D-*co*-TT) (TT/2Cz-D=10:1) films (Fig. 9(a)). With the decreasing temperature, all the Seebeck coefficients decreased gradually. Additionally, from Fig. 9(b) it can be observed that the power factors of copolymer films obtained with TT/2Cz-D=5:1 and 3:1 can be up to 0.33 μW m^{-1} K^{-2} at 303 K, relatively higher than that of PTT films. Because of their temperature dependence of electrical conductivities and Seebeck coefficients, the power factors ($P=S^2\cdot\sigma$) of all obtained polymer films gradually decreased as the temperature decreased from 300 to 200 K, as shown in Fig. 9(b). All the results indicate that as the initiate monomer feed ratio decreased from TT/2Cz-D=10:1 to 3:1, more 2Cz-D units were inserted into the copolymer main chains, which considerably improved the Seebeck coefficients of as-obtained copolymer films compared with that of PTT film, and consequently, the power factors were enhanced simultaneously.

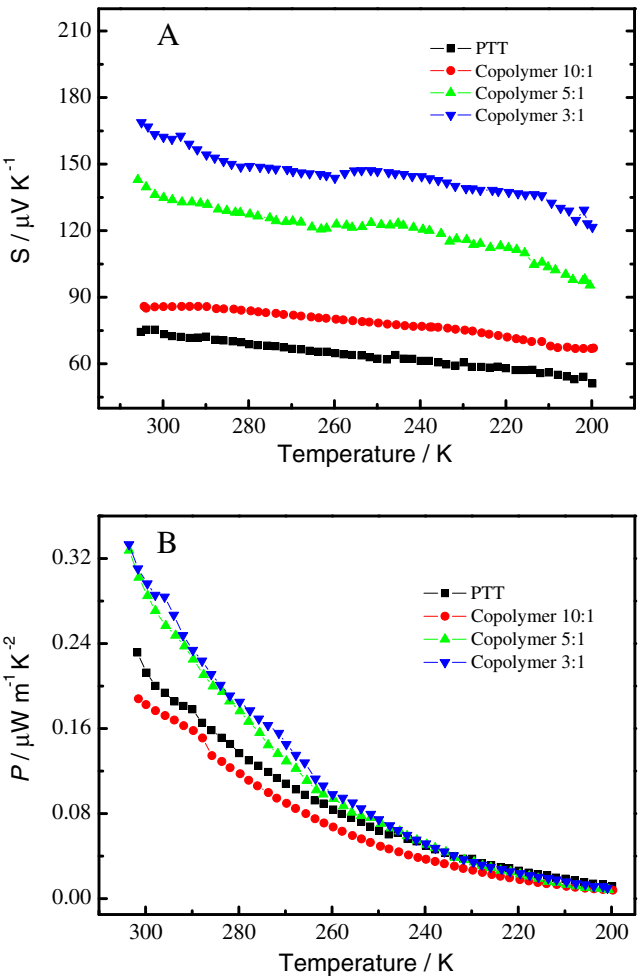

Fig. 9 Temperature dependence of Seebeck coefficient (**a**) and power factor (**b**) for PTT and copolymers synthesized with monomer feed ratios of TT/2Cz-D=10:1, 5:1, and 3:1, respectively, in BFEE + DCM (30%, vol)

However, for P2Cz-D and P(2Cz-D-*co*-TT) (TT/2Cz-D=1:3) films, there was no Seebeck effect performed, which might be attributed to their defective conjugation structures of polymer and copolymer backbone chains. Therefore, in Fig. 9 their data were not included. Because of the steric hindrance between Cz molecules and too few TT molecules presented in the mixture (TT/2Cz-D=1:3) to make up the fragmentary conjugation structures of these polymer and copolymers, the conjugation length and efficiency of as-formed P2Cz-D and P(2Cz-D-*co*-TT) (TT/2Cz-D=1:3) were limited. Thus, the carrier mobility across P2Cz-D and P(2Cz-D-*co*-TT) films was negatively affected. As the electrical conductivity σ is given by the equation: $\sigma = en\mu$ (where e, n, and μ are the electric charge, the carrier concentration, and the carrier mobility, respectively); hence, the electrical conductivities of P2Cz-D and P(2Cz-D-*co*-TT) (TT/2Cz-D=1:3) were relatively lower. A threshold value of the electrical conductivity may need to reach, until that the Seebeck effect of the material can be measured successfully. Study about the above conjecture is still in progress by our group.

Morphologies

The surface morphologies of P2Cz-D, PTT and P(2Cz-D-*co*-TT) films deposited on ITO glass surface were exhibited in Fig. 10 at a magnification of 50,000. As Fig. 10(a) shows, dense cracks can be observed at P2Cz-D film surface like dried and cracked earth, which will not give beneficial effects on the electrical conductivity of P2Cz-D film and may be another evidence for the low electrical conductivity (1.6×10^{-3} S cm^{-1}) of P2Cz-D film. Figure 10(b) shows the morphology of PTT film, it is smooth, homogeneous, and compact, thus its electrical conductivity is relatively higher (0.4 S cm^{-1}). The SEM image of the copolymer film was exhibited in Fig. 10(c), and some tiny flaws can be observed in the surface of the copolymer film, different from those of P2Cz-D (Fig. 10(a)) and PTT (Fig. 10(b)) films. Compared with P2Cz-D film, the structure and the surface morphology of the copolymer film were quite improved to give rise to the enhancement of the electrical conductivity of the copolymer film (0.19 S cm^{-1}).

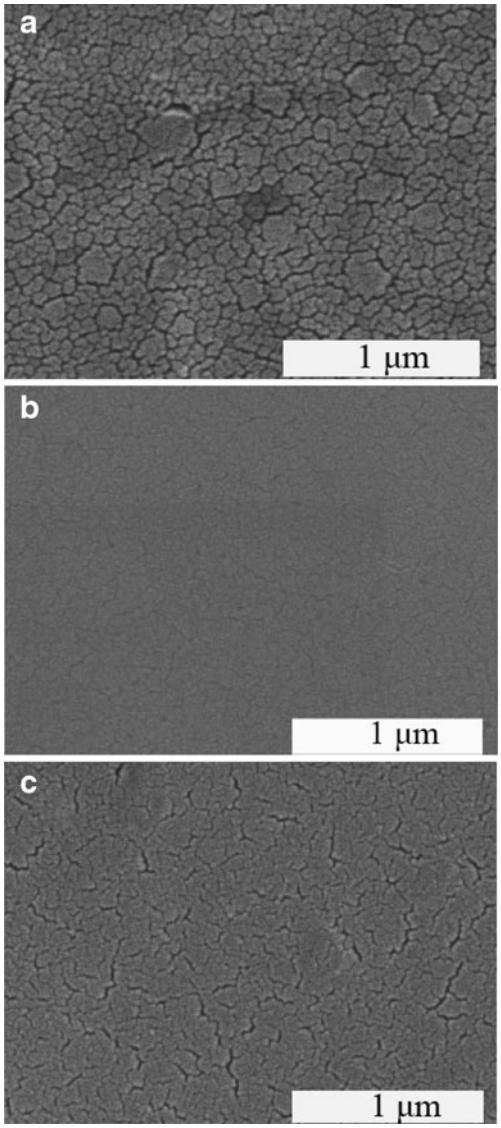

Fig. 10 SEM images of P2Cz-D (**a**), PTT (**b**), and P(2Cz-D-*co*-TT) (TT/2Cz-D=5:1) (**c**) films electrochemically synthesized in BFEE + DCM (30%, vol) on ITO glasses in doped state

Conclusions

In this study, 2Cz-D and TT were successfully copolymerized by direct anodic oxidation in BFEE containing 30% (vol) DCM. Copolymerization conditions were optimized to choose proper electrolyte and film-deposited potentials. As-formed copolymers exhibit good redox activity and stability, high mechanical property and flexibility, and relatively higher electrical conductivities. The emitting properties of obtained copolymers were studied, and they can be significantly affected by the initiate monomer feed ratios. The thermoelectric properties of as-formed polymer and copolymer films were mainly studied. Because of the presence of TT units in the copolymer backbone chains, the electrical conductivities of the copolymers were improved from 3.0×10^{-3} to 0.26 S cm^{-1} at ambient temperature as initiate monomer feed ratio increased from TT/2Cz-D=1:3 to 10:1, much higher than that of P2Cz-D (1.6×10^{-3} S cm^{-1}). On the other hand, because of the presence of 2Cz-D units in the copolymers, the Seebeck coefficients of the copolymers were enhanced from 85 to 169 μV K^{-1} at ambient temperature as the initiate monomer feed ratio decreased from TT/2Cz-D=10:1 to 3:1, much higher than

that of PTT (75 μV K^{-1}). Moreover, some obtained copolymer films exhibited higher power factors (0.33 μW m^{-1} K^{-2}) compared with that of PTT (0.23 μW m^{-1} K^{-2}). To summarize, conducting copolymer P(2Cz-D-*co*-TT) films with improved thermoelectric properties and high film-quality were successfully achieved, foretelling the promising future application as a novel organic thermoelectric material.

Acknowledgements NSFC (50963002, 51073074 and 60767001) are acknowledged for their financial supports.

References

1. Tritt TM, Bőttner H, Chen LD (2008) MRS Bull 33:366
2. Snyder GJ, Toberer ES (2008) Nat Mater 7:105
3. Yao Q, Chen LD, Zhang WQ, Liufu SC, Chen XH (2010) Nano 4:2445
4. Goldsmid HJ, Giutronich JE, Kaila MM (1980) Sol Energy 24:435
5. Chen B, Xu JH, Uher C, Morelli DT, Meisner GP, Fleurial JP, Caillat T, Borshchevsky A (1997) Phys Re B 55:1476
6. Uher C, Yang J, Hu S, Morelli DT, Meisner GP (1999) Phys Re B 59:8615
7. Nolas GS, Cohn JL, Slack GA, Schujman SB (1998) Appl Phys Lett 73:178
8. Littleton RT, Tritt TM, Feger CR, Kolis J, Wilson ML, Marone M, Payne J, Verebeli D, Levy F (1998) Appl Phys Lett 72:2056
9. Toshima N (2002) Macromol Symp 186:81
10. Pintér E, Fekete ZA, Berkesi O, Makra P, Patzkó Á, Visy C (2007) J Phys Chem C 111:11872
11. Dasaroyong K, Yeonseok K, Kyungwho C, Grunlan JC, Choongho Y (2010) Nano 4:513
12. Sun J, Yeh ML, Jung BJ, Zhang B, Feser J, Majumdar A, Katz HE (2010) Macromolecules 43:2897
13. Lévesque I, Bertrand PO, Blouin N, Leclerc M, Zecchin S, Zotti G, Ratcliffe CI, Klug DD, Gao X, Gao F, Tse JS (2007) Chem Mater 19:2128
14. Lévesque I, Gao X, Klug DD, Tse JS, Ratcliffe CI, Leclerc M (2005) React Funct Polym 65:23
15. Aïch RB, Blouin N, Bouchard A, Leclerc M (2009) Chem Mater 21:751
16. Meng CZ, Liu CH, Fan SS (2010) Adv Mater 22:535
17. Hiroshige Y, Ookawa M, Toshima N (2006) Synth Met 156:1341
18. Hiroshige Y, Ookawa M, Toshima N (2007) Synth Met 157:467
19. Kemp NT, Kaiser AB, Liu CJ, Chapman B, Mercier O, Carr AM, Trodahl HJ, Buckley RG, Partridge AC, Lee JY, Kim CY, Bartl A, Dunsch L, Smith WT, Shapiro JS (1999) J Polym Sci B Polym Phys 37:953
20. Choongho Y, Yeon SK, Dasaroyong K, Jaime CG (2008) Nano Lett 8:4428
21. Zhang B, Sun J, Katz HE, Fang F, Opila RL (2010) Appl Mater Interfaces 2:3170
22. Jia PT, Xu JW, Ma J, Lu XH (2009) Eur Polym J 45:772
23. Natori I, Natori S, Sekikawa H, Takahashi T, Sato H (2010) J Appl Polym Sci 118:69
24. Yue RR, Xu JK, Lu BY, Liu CC, Li YZ, Zhu ZJ, Chen S (2009) J Mater Sci 44:5909
25. Dang XD, Intelmann CM, Rammelt U, Plieth W (2003) J Solid State Electrochem 8:727
26. Desbene-Monvernay A, Lacaze PC, Dubois JE (1981) J Electroanal Chem 129:229
27. Lacaze PC, Dubois JE, Desbene-Monvernay A, Desbene PL, Basselier JJ, Richard D (1983) J Electroanal Chem 147:107
28. Desbene-Monvernay A, Tsamantakis A, Lacaze PC, Dubois JE (1986) J Electroanal Chem 199:449
29. Inzelt G (2003) J Solid State Electrochem 7:503
30. Reddinger JL, Sotzing GA, Reynolds JR (1996) Chem Commun 15:1777
31. Kruzinauskiene A, Matoliukstyte A, Michaleviciute A, Grazulevicius JV, Musnickas J, Gaidelis V, Jankauskas V (2007) Synth Met 157:401
32. Low PJ, Paterson MAJ, Yufit DS, Howart JAK, Cherryman JC, Tackley DR, Brook R, Brown B (2005) J Mater Chem 15:2304
33. MacClenaghan ND, Passalacqua R, Loiseau F, Campagna S, Verheyde B, Hameurlaine A, Dehaen W (2003) J Am Chem Soc 125:5356
34. Trannekar P, Fulghum T, Baba A, Patton D, Advincula R (2007) Langmuir 23:908
35. Marrec P, Dano C, Gueguen-Simonet N, Simonet J (1997) Synth Met 89:171
36. Diamant Y, Furmanovich E, Landau A, Lellouche JP, Zaban A (2003) Electrochim Acta 48:507
37. Koyuncu S, Gultekin B, Zafer C, Bilgili H, Can M, Demic S, Kaya I, Icli S (2009) Electrochim Acta 54:5694
38. Wei ZH, Wang Q, Xu JK, Nie YL, Du YK, Xia HY (2008) J Polym Sci A Polym Chem 46:5232
39. Yue RR, Chen S, Lu BY, Liu CC, Xu JK (2010) J Solid State Electrochem.
40. Li Y, Ding J, Day M, Tao Y, Lu J, Diorio M (2004) Chem Mater 16:2165
41. Fuller LS, Iddon B, Smith KA (1997) J Chem Soc Perkin Trans 1:3465
42. Game RR, Allison JL, Call RS, Coval CA (1977) J Am Chem Soc 99:7170
43. Kuwabata S, Ito S, Yoneyama H (1988) J Electrochem Soc 135:1691
44. Camurlu P, Şahmetlioğlub E, Şahinc E, Akhmedovd İM, Tanyelid C, Toppare L (2008) Thin Solid Films 516:4139
45. Otero TF, Larreta-Azelain ED (1988) Polymer 29:1522
46. Ak M, Sahmetlioglu E, Toppare L (2008) J Electroanal Chem 621:55
47. Lu BY, Yan J, Xu JK, Zhou SY, Hu XJ (2010) Macromolecules 43:4599
48. Kumar A, Welsh DM, Morvant MC, Piroux F, Abboud KA, Reynolds JR (1998) Chem Mater 10:896
49. Yang L, Dorsinville R, Wang QZ, Zou WK, Ho PP, Yang NL, Alfano RR, Zamboni R, Danieli R, Ruani G, Taliani C (1989) J Opt Soc Am B 6:753
50. Taliani C, Zamboni R, Danieli R, Ostoja P, Porzio W, Lazzaroni R, Bredas JL (1989) Phys Scr 40:781
51. Morin JF, Leclerc M, Ades D, Siove A (2005) Macromol Rapid Commun 26:761